Dependence of the thermoelectric properties of $CeFe_{3.5}Co_{0.5}Sb_{12}$ on the parameters of mechanochemical synthesis and spark plasma sintering

© K.A. Scherbakova, E.V. Chernyshova, E.V. Argunov, F.Yu. Bochkanov, A.I. Voronin, V.V. Khovaylo

National University of Science and Technology MISiS,
119049 Moscow, Russia

E-mail: m1804497@edu.misis.ru, m152292@edu.misis.ru

Received March 11, 2024
Revised March 19, 2024
Accepted March 19, 2024

p-type skutterudite of $CeFe_{3.5}Co_{0.5}Sb_{12}$ nominal composition was prepared by mechanochemical synthesis and spark plasma sintering. Compared to traditional synthesis methods, the proposed approach makes it possible to reduce the time for preparation of skutterudite thermoelectrics by more than an order of magnitude. By varying both the grinding time and the sintering temperature, it was possible to reduce the amount of secondary phases $FeSb_2$ and Sb, the presence of which has a negative effect on the Seebeck coefficient in particular and on the thermoelectric figure of merit in general. The highest value of thermoelectric figure of merit, $zT = 0.4$ at 773 K, demonstrated the sample obtained after 30 minutes of grinding and sintered at 798 K.

Keywords: *p*-type skutterudites, mechanochemical synthesis, spark plasma sintering, thermoelectric properties.

DOI: 10.61011/SC.2024.02.58358.23T

1. Introduction

Thermoelectric (TE) materials have significant potential for applications in alternative energy source technology, namely in devices for direct conversion of thermal energy into electrical energy [1,2]. The efficiency of TE materials is characterized by a dimensionless thermoelectric figure of merit zT, defined as $zT = S^2\sigma T/\kappa$, where S, σ and κ — the Seebeck coefficient, electrical conductivity and total thermal conductivity ($\kappa = \kappa_{el} + \kappa_{lat}$, where κ_{el} and κ_{lat} — electronic and lattice contributions, respectively) of the material, and T — the absolute temperature [3]. Increasing the zT of TE materials is an unconventional task since S, σ and κ represent interdependent characteristics of solids. A common strategy is to reduce thermal conductivity, while maintaining high values of the Seebeck coefficient and electrical conductivity.

The filled skutterudites are considered to be one of the most highly efficient TE materials in the medium temperature range [4]. The high figure of merit of these compounds is primarily attributable to the fact that this type of materials implement the concept of „phonon glass — electron crystal“ (PGEC) [5], which makes it possible to independently optimize the electro- and thermophysical properties. The general formula of filled skutterudites is $R_xT_4Pn_{12}$, where R is a filler (rattler), which are mainly alkaline or alkaline earth metals, as well as lanthanides and actinoids, T is a transition metal, and Pn is a pnictogen. Commonly, x, which indicates the degree of filling of octahedral voids of the crystal lattice with rattlers, strongly depends on the chemical composition of skutterudites and does not exceed 0.3 for compounds with T = Co. The latest research shows that, the values of zT in *n*-type skutterudites based on $CoSb_3$ reach ~ 1.80 if two or three different rattlers are added [6–9], whereas the values of zT in *p*-type skutterudites mostly remain below 1 [10–12]. The improvement of the TE properties of skutterudites compound of *p*-type is a crucial task considering that TE modules require both *n*- and *p*-type materials with comparable characteristics.

Since skutterudites are among the most prominent representatives of the Zintl phases, the stability of which is determined by the number of valence electrons [13], Co_4Sb_{12} is a stable compound, since it has 96 valence electrons. Skutterudite Fe_4Sb_{12}, which has 92 valence electrons, is a metastable compound. However, it is possible to stabilize iron-based skutterudite compounds by partially replacing Fe with Co or filling octahedral voids, for example, with lanthanides. It is worth noting that the limit proportion of filling of x voids decreases with an increase of the cobalt content, which in compounds based on Fe_4Sb_{12} is equal to 1, and it is usually lower than 0.3 in skutterudites with T = Co. The optimal approach for stabilizing Fe-based skutterudites is both the Fe/Co partial substitution and the introduction of rattlers into octahedral voids of the crystal structure.

Significant efforts of researchers are also aimed at finding new, more efficient methods for producing skutterudites, which reduce time and energy costs for sample synthesis. Typically, skutterudite compounds are produced by prolonged and energy-consuming methods; for example, melting, quenching, long-term annealing and subsequent spark plasma sintering (SPS) [14]. It takes about 9 days and requires significant energy to obtain a sample.

In this regard, the purpose of this paper is to study and develop a method for producing *p*-type filled skutterudite

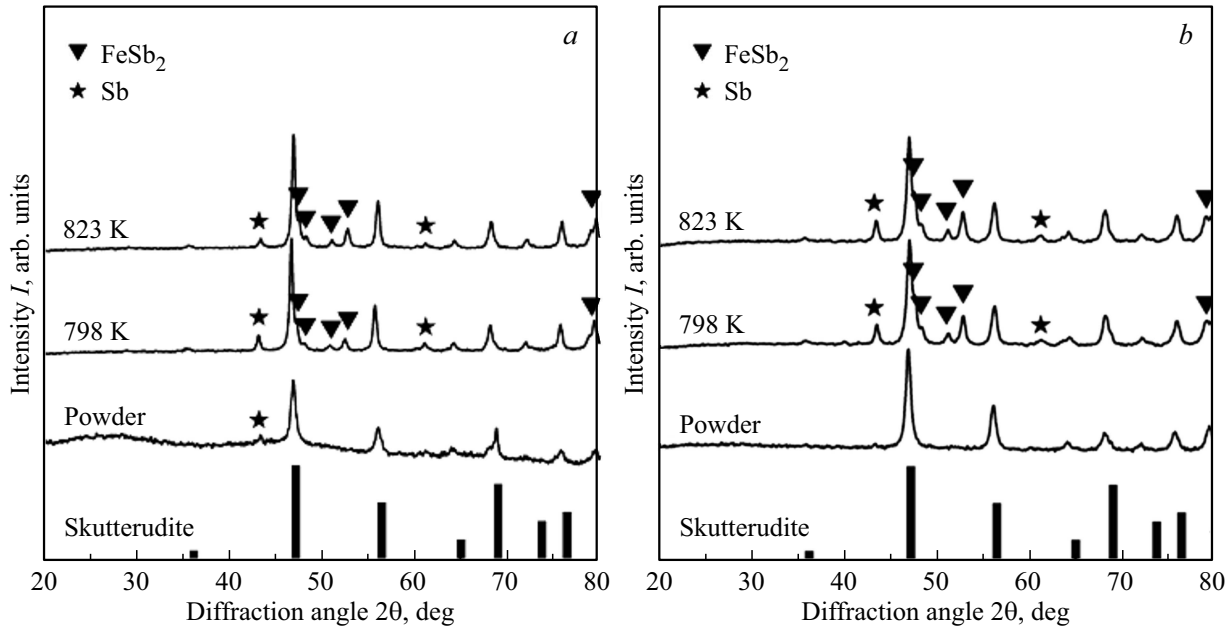

Figure 1. Diffractograms of powder and bulk samples (798 and 823 K): *a* — after 30 min of MS and various sintering temperatures and *b* — after 60 min of MS and various sintering temperatures.

of $CeFe_{3.5}Co_{0.5}Sb_{12}$ chemical composition which includes mechanochemical synthesis (MS) and SPS and to observe its TE properties.

2. Experiment details

Powders of pure chemical elements: Ce (99.99%), Fe (99.99%), Co (99.99%) and Sb (99.99%) were used as starting materials. Stoichiometric quantities of the initial elements were weighed and loaded into the drums of a planetary ball mill inside a glove box under high-purity argon atmosphere ($O_2 < 0.1$ ppm, $H_2O < 5$ ppm). The MS was performed in a planetary ball mill („Aktivator 2S“, CJSC „Aktivator“) for 30 and 60 min at a speed of 694 rpm. Next, the SPS of the obtained powders („Labox 650“, Sinter Land INC.) was performed at 798 and 823 K for 10 min in a graphite mold with a diameter of 12.7 mm under pressure of 50 MPa with a heating and cooling rate of 50 and 30 K/min accordingly, under high-purity argon atmosphere ($O_2 < 0.1$ ppm, $H_2O < 5$ ppm). All samples were annealed in quartz tubes in a furnace („Carbolite“ CTF 12/65/550) at 773 K for 6 h for relieving of the internal stresses.

The phase composition of the samples was determined by powder X-ray diffraction („Diffray-401“) using CrK_α radiation ($\lambda = 0.2291$ nm). The energy dispersion spectroscopy (EDX, Oxford Inst.) was used to investigate the chemical composition of all samples. The Seebeck coefficient (S) and electrical conductivity (σ) were measured by a differential and four-contact methods, respectively (LLC „KRIOTEL“) under inert gas atmosphere. The thermal conductivity (κ) was calculated from the thermal diffusivity (α), heat capacity (C_p) and density (ρ) using the equation $\kappa = \alpha \cdot C_p \cdot \rho$. The thermal diffusivity was measured by the laser flash method (LFA 457, Netzsch), and the heat capacity was estimated using the Debye model. The density of bulk samples was measured using the Archimedes method. A porosity correction was applied according to the Maxwell–Oiken equation for processing experimental data (σ and κ), since the relative density of all samples was 91–94% [15]. Errors of the measurement of the Seebeck coefficient, electrical conductivity and thermal conductivity were within 8% for each measured value. All measurements were performed in the temperature range from 323 to 773 K.

3. Discussion of results

Figure 1 shows diffractograms of powders after MS and bulk samples of skutterudites of $CeFe_{3.5}Co_{0.5}Sb_{12}$ composition obtained by SPS. The diffraction peaks of all samples correspond to the standard data for the skutterudite phase. However, impurity phases represented by marcasite ($FeSb_2$) and antimony (Sb) were found in all samples. It is worth noting that the absence of secondary phases containing cerium suggests that Ce filled the octahedral voids of the skutterudite crystal lattice. The comparison of the amount of secondary phases in the samples depending on the grinding time showed that after 30 min their number is significantly less than after 60 min. This is attributable to the fact that a ground material is formed from the walls of steel drums as a result of a long synthesis process and the equilibrium in the system shifts towards the formation

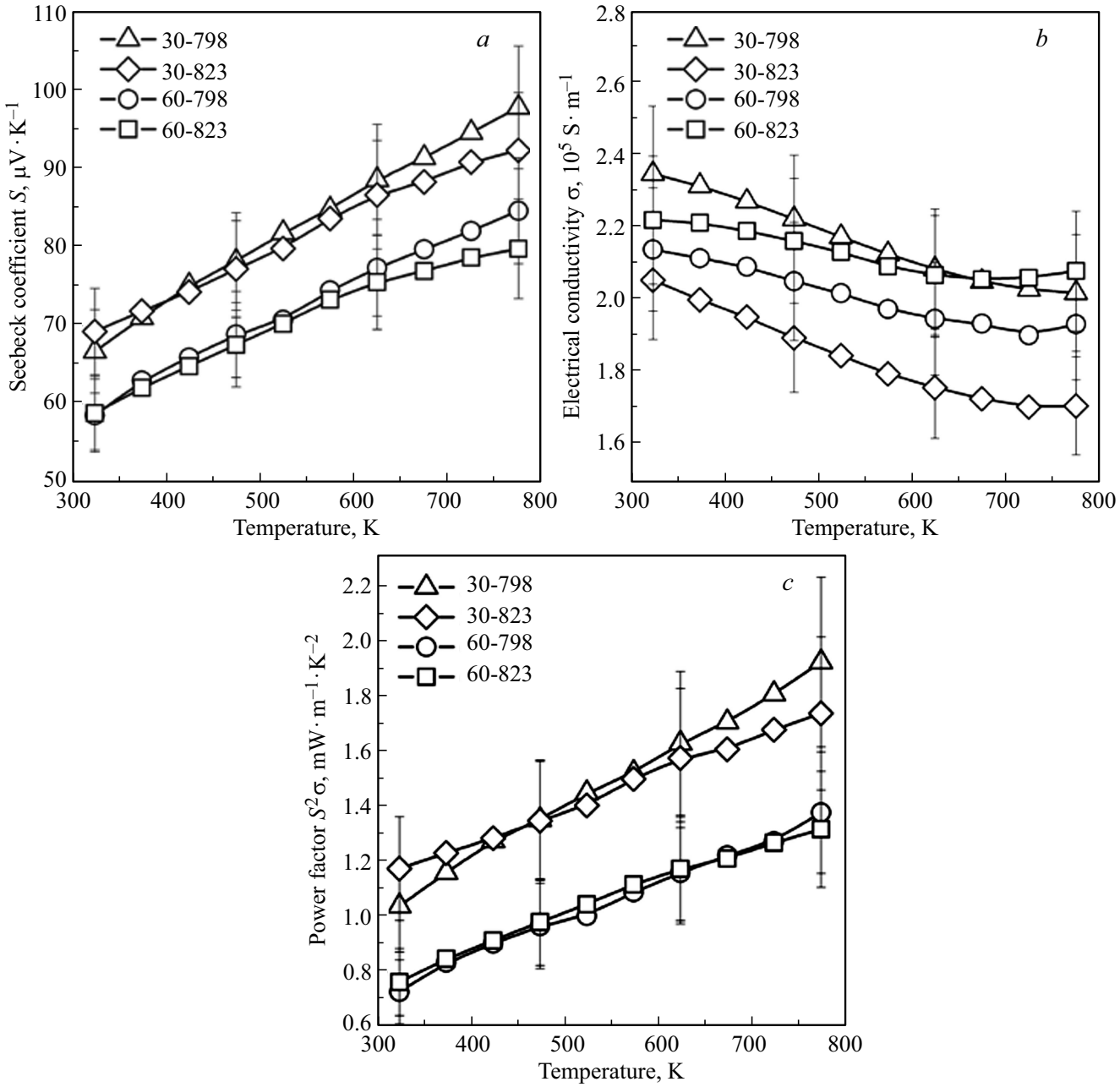

Figure 2. The temperature dependences of the Seebeck coefficient (*a*), electrical conductivity (*b*) and power factor (*c*) in $CeFe_{3.5}Co_{0.5}Sb_{12}$.

of $FeSb_2$ due to the presence of excess iron. The SPS temperature impacts on the number of impurity phases: at 798 K it is $\sim$ 5% less than in the sample sintered at 823 K.

Based on the analysis of the obtained diffractograms, the main phase is formed both during synthesis and sintering of the sample, which is observed in the case of „reactive" spark plasma sintering [16].

A specific number is assigned to each sample in Table 1 for the convenience of further consideration of TE properties. The nominal and actual compositions of the synthesized samples are presented in Table 2. The absence of Ce-containing impurity phases indicates that Ce fills the octahedral voids of the crystal structure. The deviation of the values of other elements from the nominal composition is attributable to the formation of secondary phases.

Figure 2, *a* shows the temperature dependence of the Seebeck coefficient S for $CeFe_{3.5}Co_{0.5}Sb_{12}$. All samples have positive values of S over the entire observed temperature range, which indicates that the main charge carriers in the studied compounds are holes. The Seebeck coefficient increases linearly up to $T \sim 600$ K. Obviously, the phase composition has a decisive impact on the values obtained. It is worth noting that samples after 60 min of grinding show lower values of the Seebeck coefficient because of a

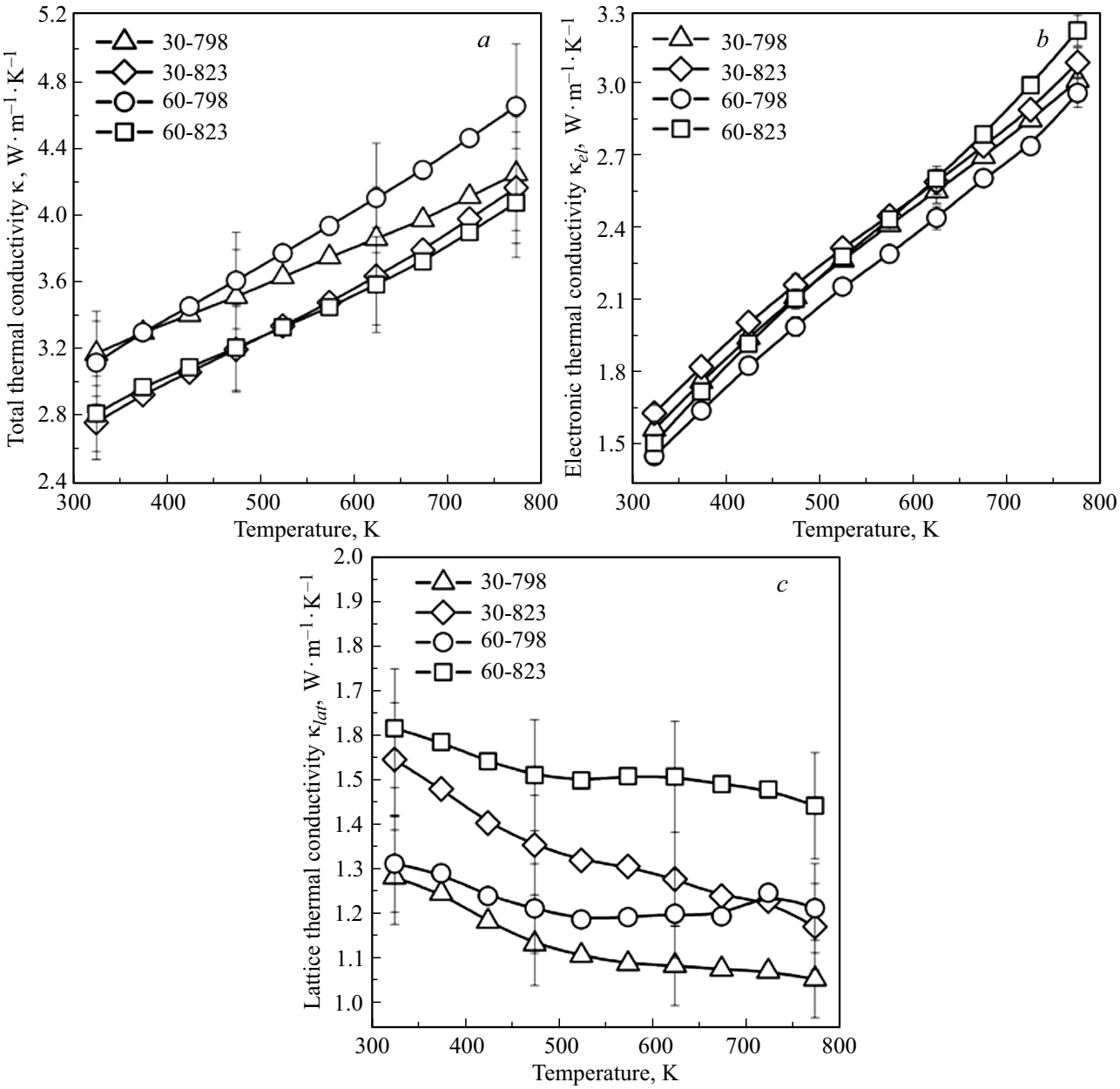

Figure 3. The temperature dependences of the total (*a*), electronic (*b*) and lattice (*c*) thermal conductivity of $CeFe_{3.5}Co_{0.5}Sb_{12}$.

Table 1. The samples of the $CeFe_{3.5}Co_{0.5}Sb_{12}$ composition are numbered depending on synthesis parameters

Time MS	SPS Temperature	Sample Number
30 min	798 K	30-798
	823 K	30-823
60 min	798 K	60-798
	823 K	60-823

Table 2. Nominal and actual composition of synthesized bulk samples

Number Sample	Nominal Composition	Actual Composition
30-798	$CeFe_{3.5}Co_{0.5}Sb_{12}$	$Ce_{0.97}Fe_{3.54}Co_{0.37}Sb_{12.12}$
30-823		$Ce_{1.00}Fe_{3.26}Co_{0.56}Sb_{12.17}$
60-798		$Ce_{0.99}Fe_{3.61}Co_{0.47}Sb_{11.92}$
60-823		$Ce_{0.94}Fe_{3.17}Co_{0.57}Sb_{12.31}$

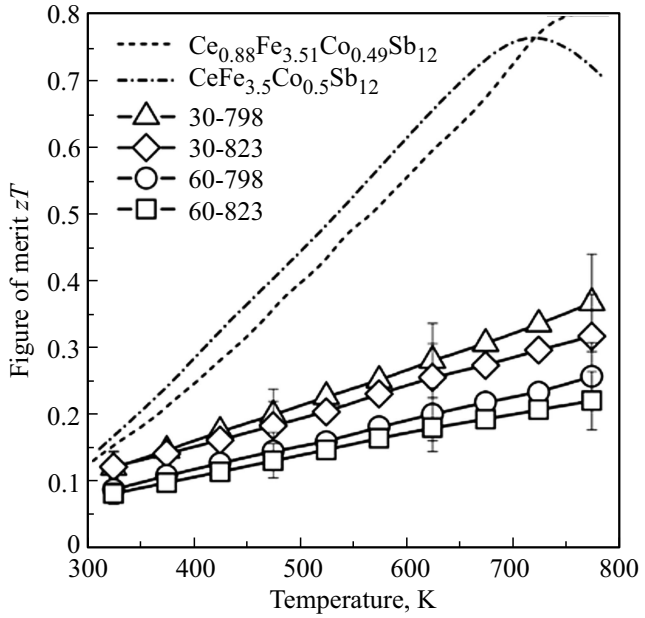

Figure 4. Temperature dependence of the thermoelectric figure of merit. The literature data are given for $Ce_{0.88}Fe_{3.51}Co_{0.49}Sb_{12}$ [20] and $CeFe_{3.5}Co_{0.5}Sb_{12}$ [20].

larger number of impurity phases. The sintering temperature does not have a significant impact on S, since the difference in S for samples sintered at different temperatures is within the measurement error. The sample 30-798 at 773 K has maximum value of the Seebeck coefficient $97.7\,\mu\mathrm{V}\cdot\mathrm{K}^{-1}$.

The temperature dependence of the electrical conductivity of synthesized bulk materials is shown in Figure 2, *b*. It is worth noting that all samples demonstrate the metallic conductivity characteristic of degenerate semiconductors. At the same time, the electrical conductivity of the obtained samples is higher than the values for these compounds obtained by the traditional method [17,18], which is attributable to the greater volume fraction of secondary phases ($FeSb_2$ and Sb). The sample 30-798 has the highest values of electrical conductivity of $(2.35–2.05)\cdot 10^5\,\mathrm{S}\cdot\mathrm{m}^{-1}$ in the temperature range up to 673 K.

The temperature dependences of the power factor $PF = S^2\sigma$ is shown in Figure 2, *c*. The dependences of PF and S on temperature do not differ qualitatively since $PF \sim S^2$ and the absolute variation of the electrical conductivity are significantly less than the absolute change S. The maximum value of $PF = 1.93\,\mathrm{mW}\cdot\mathrm{m}^{-1}\cdot\mathrm{K}^{-2}$ is observed in the sample 30-798.

Figure 3, *a* shows the temperature dependence of the total thermal conductivity (κ) for all samples of $CeFe_{3.5}Co_{0.5}Sb_{12}$. The values of κ increase with the increase of temperature in the entire studied range. The total thermal conductivity κ is the sum of two contributions: lattice (κ_{lat}) and electronic (κ_{el}). κ_{el} can be estimated using the formula $\kappa_{el} = L\cdot\sigma\cdot T$ according to the Wiedemann–Franz law, where L is the Lorentz number. Therefore, κ_{lat} can be calculated as $\kappa_{lat} = \kappa - \kappa_{el}$. The temperature dependence κ_{el} for all samples is shown in Figure 3, *b*. The electronic contribution of thermal conductivity increases over the entire temperature range due to an increase in the average thermal energy of charge carriers. The sample 60-823 demonstrates the smallest values of $\kappa_{el} = 1.45–2.96\,\mathrm{W}\cdot\mathrm{m}^{-1}\cdot\mathrm{K}^{-1}$ (Figure 3, *b*). Figure 3, *c* shows the temperature dependence κ_{lat} of samples. The lattice contribution of thermal conductivity gradually decreases with the increase of the temperature, which is mainly due

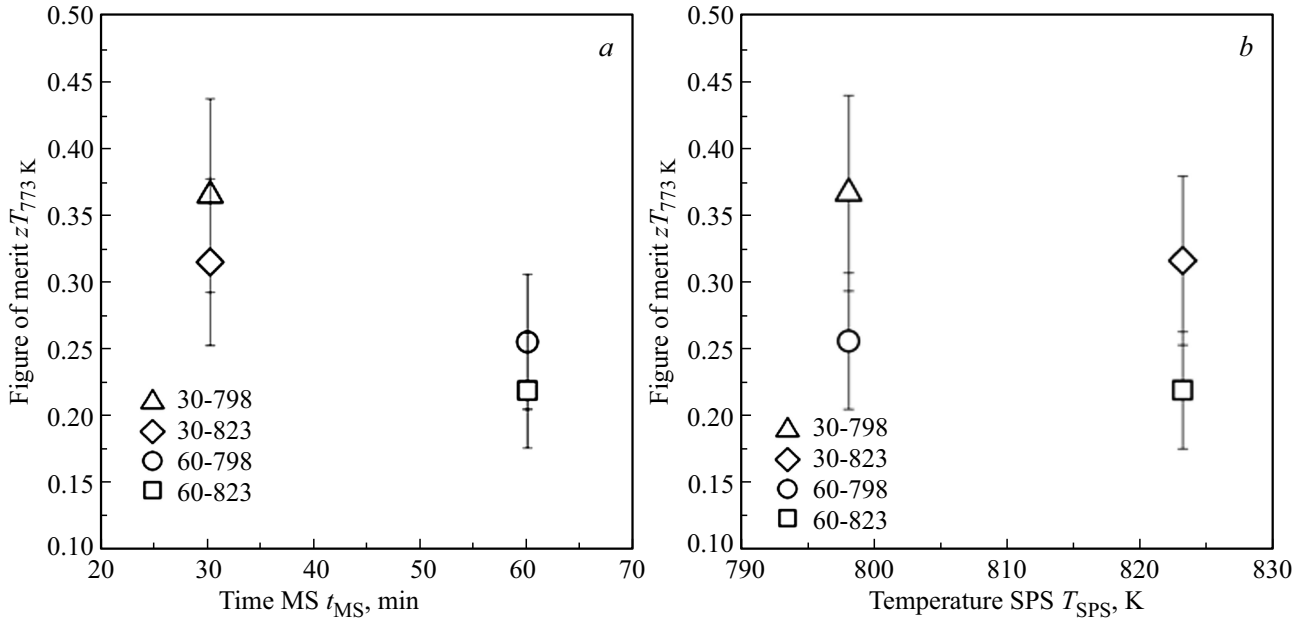

Figure 5. Dependence of the thermoelectric figure of merit of the samples at 773 K on the time MS (*a*) and on the temperature of SPS (*b*).

to phonon-phonon scattering. The sample 30-798 demonstrates the lowest values of $\kappa_{lat} = 1.28-1.05\,\mathrm{W}\cdot\mathrm{m}^{-1}\cdot\mathrm{K}^{-1}$ in the entire temperature range. The ambiguous dependence of thermal conductivity (Figure 3, *a*) is also observed due to the complex relationship with the microstructure and phase composition of the samples. The smallest amount of phase $FeSb_2$ was found in the sample 30-798, which is characterized by high thermal conductivity, which causes the smallest κ_{lat}.

The temperature dependence of the figure of merit zT is shown in Figure 4. zT of the samples increases linearly with the increase of temperature, reaching maximum at 773 K in the presented temperature range. The sample 30-798 has maximum value of $zT = 0.4$. For comparison, Figure 4 also presents data for compounds of similar composition synthesized by longer and more energy-consuming methods, such as synthesis at high pressures [19], where $zT \sim 0.8$ was obtained at 763 K, or solid-phase synthesis [20], where zT reached values of ~ 0.78 at 750 K.

Figure 5 shows the dependences of the values of zT at 773 K on the time of MS (Figure 5, *a*) and on the temperature of the SPS (Figure 5, *b*) for the analysis of the effect of synthesis parameters on the final values of the figure of merit of the samples. Based on the graphs, it can be concluded that the synthesis time has a more significant effect on the samples than the sintering temperature. zT decreases $\sim 30\%$ with an increase of the grinding time from 30 to 60 min, and zT decreases only $\sim 14\%$ with an increase of the sintering temperature from 798 to 823 K.

4. Conclusion

This paper presents a method for obtaining $CeFe_{3.5}Co_{0.5}Sb_{12}$ skutterudite of *p*-type using mechanochemical synthesis and spark plasma sintering. Structural studies indicate that the formation of the skutterudite phase occurs both during mechanochemical synthesis and during spark plasma sintering. The content of secondary phases of $FeSb_2$ and Sb can be reduced by varying the parameters of obtaining both powder and bulk material. The highest values of thermoelectric figure of merit $zT \sim 0.4$ were achieved in the sample obtained after 30 min of mechanochemical synthesis and sintered at a temperature of 798 K. The proposed synthesis method makes it possible to obtain bulk samples of skutterudite of *p*-type in less than 10 h, which distinguishes it from traditional synthesis methods, where the synthesis of similar materials takes 5–7 days. However, the synthesized samples have a lower (~ 2 times) thermoelectric figure of merit compared to the record values of zT, which were reported in the literature [19,20]. The decrease of thermoelectric figure of merit in the samples is attributable to the presence of secondary phases of $FeSb_2$ and Sb, which reduce the Seebeck coefficient and, in some cases, increase thermal conductivity. Further optimization of the parameters of both mechanochemical synthesis and spark plasma sintering will reduce the proportion of secondary phases and thus significantly increase the zT of this type of materials.

Funding

This research was supported financially by the Russian Science Foundation (grant No. 19-79-10282-P).

Conflict of interest

The authors declare that they have no conflict of interest.

References

[1] D.M. Rowe (ed.). *Thermoelectrics Handbook: Macro to Nano* (Boca Raton, CRC Press, 2006).
[2] L.E. Bell. Science, **321**, 1457 (2008).
[3] A.F. Ioffe. *Poluprovodnikovye elementy* (M.-L., Izd-vo AN SSSR, 1956). (in Russian).
[4] C. Uher (ed.). *Modules, Systems, and Applications in Thermoelectrics* (Boca Raton, CRC Press, 2012).
[5] G.A. Slack (ed.). *Handbook of Thermoelectricity* (Boca Raton, CRC Press, 1995) p. 407.
[6] J.Y. Jung, K.H. Park, I.H. Kim. J. Kor. Phys. Soc., **57**, 773 (2010).
[7] W. Zhao, Q. Zhang, C. Dong, L. Liu, X. Tang. J. Am. Chem. Soc., **131**, 3713 (2011).
[8] J. Graff, S. Zhu, T. Holgate, J. Peng, J. He, T.M. Tritt. J. Electron. Mater., **40**, 696 (2011).
[9] G. Rogl, A. Grytsiv, K. Yubuta, S. Puchegger, E. Bauer, C. Raju, R.C. Mallik, P. Rogl. Acta Mater., **95**, 201 (2015).
[10] G.J. Tan, S.Y. Wang, Y.G. Yan, H. Li, X.F. Tang. J. Electron. Mater., **41**, 1147 (2012).
[11] J. Yu, W.Y. Zhao, P. Wei, D.G. Tang, Q.J. Zhang. J. Electron. Mater., **41**, 1414 (2012).
[12] R. Liu, X. Chen, P. Qiu, J. Liu, J. Yang, X. Huang, L. Chen. J. Appl. Phys., **109** (2), 023719 (2011).
[13] H. Luo, J. W. Krizan, L. Muechler, N. Haldolaarachchige, T. Klimczuk, W. Xie, J.R. Cava. Nature Commun., **6** (1), 6489 (2015).
[14] Z. Liu, W. Zhu, X. Nie, W. Zhao. J. Mater. Sci.: Mater. Electron., **30**, 12493 (2019).
[15] A. Eucken. Forschung auf dem Gebiet des Ingenieurwesens A, **11**, 6 (1940).
[16] A. Novitskii, I. Serhiienko, S. Novikov, K. Kuskov, D. Pankratova, T. Sviridova, V. Khovaylo. J. Alloys Compd., **912**, 165208 (2022).
[17] G.J. Tan, S.Y. Wang, Y.G. Yan, H. Li, X.F. Tang. J. Electron. Mater., **41**, 1147 (2012).
[18] G. Tan, W. Liu, S. Wang, Y. Yan, H. Li, X. Tang, C. Uher. J. Mater. Chem. A, **1** (40), 12657 (2013).
[19] Y. Liu, X. Li, Q. Zhang, L. Zhang, D. Yu, B. Xu, Y. Tian. Materials, **9** (4), 257 (2016).
[20] J. Kim, Y. Ohishi, H. Muta, K. Kurosaki. AIP Advances, **8** (10), 105104 (2018).

Translated by A.Akhtyamov